Preprints (www.preprints.org) | NOT PEER-REVIEWED | Posted: 18 December 2017 doi:10.20944/preprints201712.0113.v1

Peer-reviewed version available at *Fluids* **2018**, *3*, 10; doi:10.3390/fluids3010010

Article

Design of a Novel μ-Mixer

Athanasios G. Kanaris[2], Aikaterini A. Mouza[1]*

[1] Department of Chemical Engineering, Aristotle University of Thessaloniki, Greece
[2] Scientific Computing Department, STFC, Rutherford Appleton Laboratory, Didcot, UK
* Correspondence: mouza@auth.gr; Tel.: +30 2310 994161

Abstract: In this work the efficiency of a new μ-mixer design is investigated. As in this type of devices the Reynolds number is low, mixing is diffusion dominated and it can be enhanced by creating secondary flows. In this study we propose the introduction of helical inserts into a straight tube to create swirling flow. The influence of the insert's geometrical parameters (pitch and length of the propeller blades) and of the Reynolds number on the mixing efficiency and on the pressure drop are numerically investigated. The mixing efficiency of the device is assessed by calculating a number, i.e. the Index of Mixing Efficiency that quantifies the uniformity of concentration at the outlet of the device. The influence of the design parameters on the mixing efficiency is assessed by performing a series of "computational" experiments, in which the values of the parameter are selected using DOE methodology. Finally using the numerical data, appropriate design equations are formulated, which, for given values of the design parameters, can estimate with reasonable accuracy both the mixing efficiency and the pressure drop of the proposed mixing device.

Keywords: mixing; CFD; microfluidics

1 Introduction

The increasing demand for more economical and, at the same time, more environmentally friendly production methods has led to the design of new process equipment. By the term micro-device (μ-device) we refer to devices with at least one characteristic dimension of the order of a few millimeters. Key benefits of μ-devices are the development of energy friendly, productive and cost-effective performance processes which at the same time provide greater security. For example, μ-reactors, i.e., devices with characteristic dimensions in the submillimeter range, offer significant advantages over conventional reactors, such as increased safety and reliability, as well as better process control and scalability. Due to the small characteristic dimension of the conduit, the flow in μ-reactors is laminar. As the extent of the chemical reactions is governed by the slow diffusive mass transfer, which in turn is proportional to the interfacial area between the reacting phases, the μ-reactor design turns to be a μ-mixer design problem. That is why mixing in the small devices is studied extensively in recent years.

Depending on the way mixing is enhanced, μ-mixers are distinguished in passive and active ones. In active μ-mixers, an external source of energy is used. Active micromixers are unfortunately difficult to integrate and have in general a higher implementation cost. In passive μ-mixers, whose key advantage is the low operating cost, mixing efficiency is enhanced by incorporating parts that promote secondary flows (e.g. curved sections, backward or forward facing steps). Several comprehensive reviews of μ-mixing devices and their principles can be found in the relevant literature [1-5].

In previous work in our Laboratory the mixing efficiency of several types of passive μ-mixers was investigated both experimentally and numerically [5-7]. Figure 1 shows common types of passive μ-mixers (i.e. Dean-type [6, 7] and L-type [5]) whose functional characteristics were studied in our previ-

© 2017 by the author(s). Distributed under a Creative Commons CC BY license.

Preprints (www.preprints.org) | NOT PEER-REVIEWED | Posted: 18 December 2017 doi:10.20944/preprints201712.0113.v1

Peer-reviewed version available at Fluids 2018, 3, 10; doi:10.3390/fluids3010010

ous works. Static mixers that create swirl flow are common in the macro scale and recently the application of swirl inducing configurations has been also studied in the μ-scale [8]. Moreover it is suggested [9] that the addition of obstructions as part of the channel geometry can be also beneficial to micromixer efficiency.

As it has been reported [3, 7] mixing can be improved by "chaotic advection", which involves breaking, stretching, and folding of liquid streams leading to an increase of the interfacial contact area of the fluids. It is also known [10] that static helical mixers are widely used in the chemical industry for in-line blending of liquids under laminar flow conditions and also that the geometric modification of their elements can significantly improve their mixing performance.

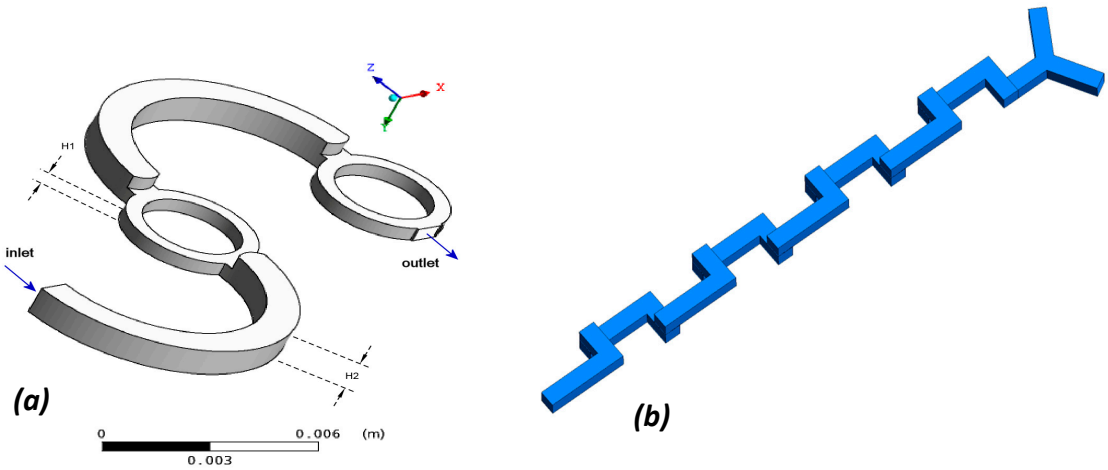

Figure 1: Common types of passive μ-mixer: a) Dean-type [6, 7] & b) *L*-type [5].

Motivated by the above, the **purpose** of this study is to investigate the possibility of using a helical insert (Figure 2) that enhances mixing by generating swirl flow. More precisely, our aim is to numerically assess the effect of the geometric parameters of the helical insert (pitch and length of the insert blades) (Figure 3) as well as the physical properties of the fluids to be mixed on both the mixing efficiency of the mixing device and the resulting pressure drop.

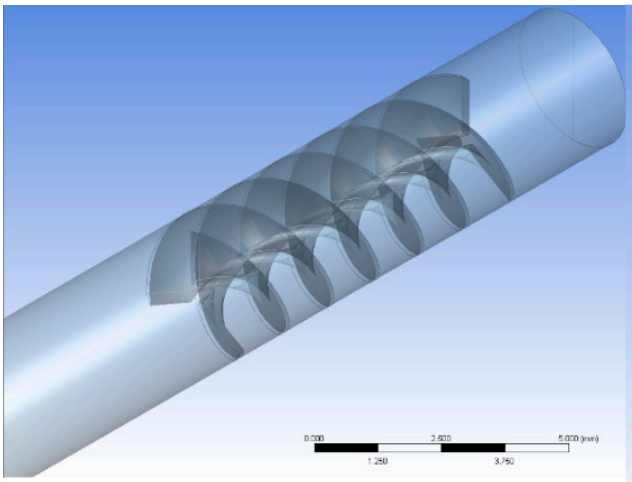

Figure 2: Schematic of the μ-mixer.

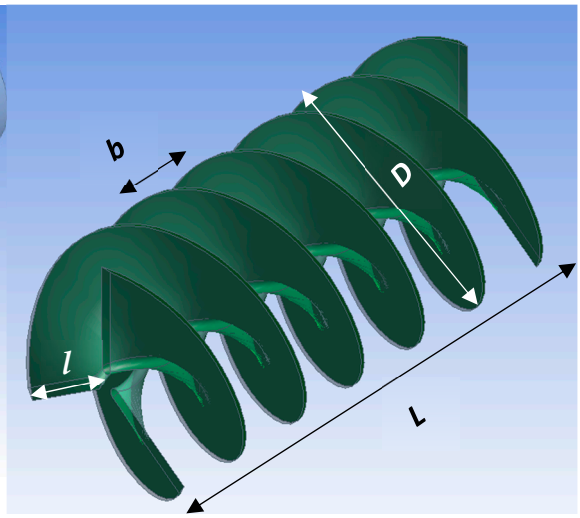

Figure 3: Geometry of the swirl generator insert.

2 Numerical Methodology

The velocity field was visualized using a *CFD* code (*ANSYS CFX 18.1*) while the computational geometry and the mesh were designed using the parametric features of ANSYS Workbench package. The μ-channel was modeled as a 3D computational domain. The simulations are performed using the

Preprints (www.preprints.org) | NOT PEER-REVIEWED | Posted: 18 December 2017 doi:10.20944/preprints201712.0113.v1

Peer-reviewed version available at Fluids 2018, 3, 10; doi:10.3390/fluids3010010

ANSYS-CFX code, which includes the usual parts of a standard CFD code. The flow domain, constructed using the Geometry section of the code, is presented in Figure 4. A grid dependency study was performed for choosing the optimum grid density. Detail of the insert is shown in Figure 4b, while the geometrical characteristics of the apparatus appear in Table 1.

Table 1: Geometrical parameters of the mixing device.

Parameter	Value
Total length of the mixer, L_m	36 mm
Internal diameter of the mixer, D_m	3.1 mm
Diameter of the insert, D	3.0 mm
Position of the insert (distance from mixer inlet), e	3.0 mm
Length of the insert, L	7.5 mm
Angle between blades, ϕ	120°
Blade length, l	0.6 to 1.74 mm
Blade pitch, b	0.625 -2.75 mm

In the present calculations, the computational fluid dynamics code uses the laminar flow model of ANSYS CFX and the high-resolution advection scheme for the discretization of the momentum equations. A pressure boundary condition of atmospheric pressure is set on the outlet port, while the convergence criterion is the mass-balance residual value to be less than 10^{-9}.

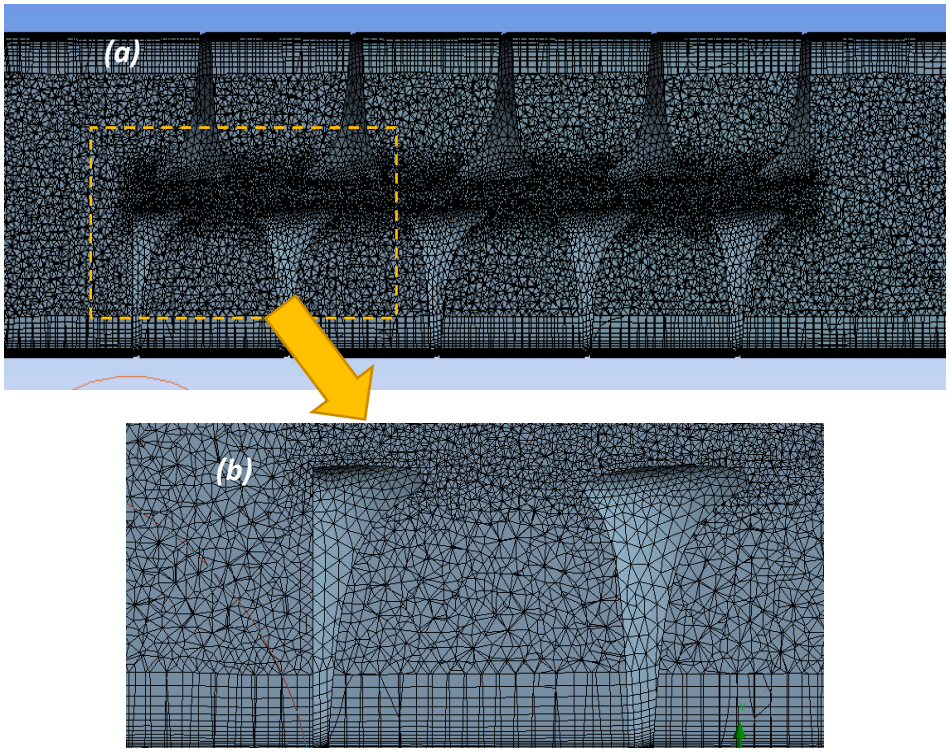

Figure 4: a) The flow domain and the grid and b) grid detail.

As the numerical diffusion in the CFD calculations can influence the accuracy of the calculations, a thorough grid dependency study was performed to ensure that the solution is independent of the grid density. The final grid parameters (minimum/maximum element size, number of divisions for the sweep mesh areas etc.) for a representative screening run were used to define the meshing parameters for the rest of the simulation runs. Number of elements for all cases varied between 850,000 and

Preprints (www.preprints.org) | NOT PEER-REVIEWED | Posted: 18 December 2017 doi:10.20944/preprints201712.0113.v1

Peer-reviewed version available at Fluids 2018, 3, 10; doi:10.3390/fluids3010010

3,000,000 elements, approximately. Due to the small characteristic dimension of the conduit the flow is laminar (Re = 9-100) and hence the laminar flow model was selected. The boundary conditions imposed are:

- velocities of the two fluids, on each of the two semicircles comprising the inlet,
- non-slip boundary condition at all walls,
- zero relative pressure at the outlet.

Moreover and for the sake of simplicity, it was assumed that one of the fluids, the base fluid, has the properties of water, while the diffusion coefficient between the two fluids equals the self-diffusion coefficient of water ($1x10^{-9}$ m^2/s).

Design parameters are declared as a mix of geometrical parameters and physical properties. Two geometrical design parameters, namely the number of turns, n, of the blade within the limits of the length of the insert, and the ratio, l/D, are used. The other variables applied are the ratios of density and dynamic viscosity for the two different mixing fluids as well as the ratio of their velocities at the entrance of the conduit. The finite volume method, a fully coupled solver for the pressure and velocity coupling, and the "high order" method to distinguish the momentum equations, all provided by ANSYS CFX, are used in the solver definition section [11]. Simulations were performed with a number of iterations that ensure a satisfactory reduction in residual mass and momentum (10^{-12}).

The mixing efficiency over a cross-section $\boldsymbol{A}$ was quantified by calculating the Index of Mixing Efficiency, I_{ME}, proposed by Kanaris et al [5], which is based on the standard deviation of mass fraction from the mean concentration over a cross section:

$$I_{ME} = 1 - \frac{\sqrt{\int_A (c-\bar{c})^2 dA}}{\sqrt{\int_A (\bar{c})^2 dA}} \quad (1)$$

where c is the mass fraction of the base fluid, in our case the water, in each cross-section unit (i.e., each grid element) and $\bar{c}$ is the mean concentration of the same fluid over the whole cross-sectional area, A, of the device. Complete mixing is achieved when the volume fraction of the base fluid in each cross-section unit equals its mean mass fraction, $\bar{c}$, which must be calculated for each individual fluid pair by taking into account their density values of the mixing fluids:

$$\text{also} \bar{c} = \frac{1}{1 + \frac{\rho}{\rho_w}} \quad (2)$$

A value of I_{ME}=1 denotes perfect mixing, i.e. the variance from the optimal mass fraction is zero.

3 Results

3.1. Screening Experiments

To assess the effect of geometrical parameters on mixing efficiency, preliminary simulations, i.e. screening experiments, were performed. For the sake of simplicity, in these simulations both fluids had the properties of water. Initially **only one** helical insert was used and the simulations revealed that the length of the fluid path after the exit of the insert has only marginal contribution to the overall efficiency of the μ-mixer. Thus, to further improve mixing efficiency, a **second insert** was placed downstream and adjacent to the first one (Figure 5). The geometrical characteristics of the two inserts are identical except that the blades of the two insert drive the fluid to opposite directions.

One of the initial screening runs, where the mixing fluids have identical properties and inlet velocities, while n=3 and l/D=0.2, is used to generate the typical results presented in Figures 5-8. In Figure 5 the flow pattern (streamlines) along the proposed device with the two inserts is presented. It is evident that the addition of the second insert improves mixing. The effect of this addition is more clearly illustrated in Figure 6, where the mass fraction distribution of the base fluid is presented at three cross sections of the device, more precisely at the exit of the first and the second insert as well as at the outlet of the device.

Preprints (www.preprints.org) | NOT PEER-REVIEWED | Posted: 18 December 2017 doi:10.20944/preprints201712.0113.v1

Peer-reviewed version available at Fluids 2018, 3, 10; doi:10.3390/fluids3010010

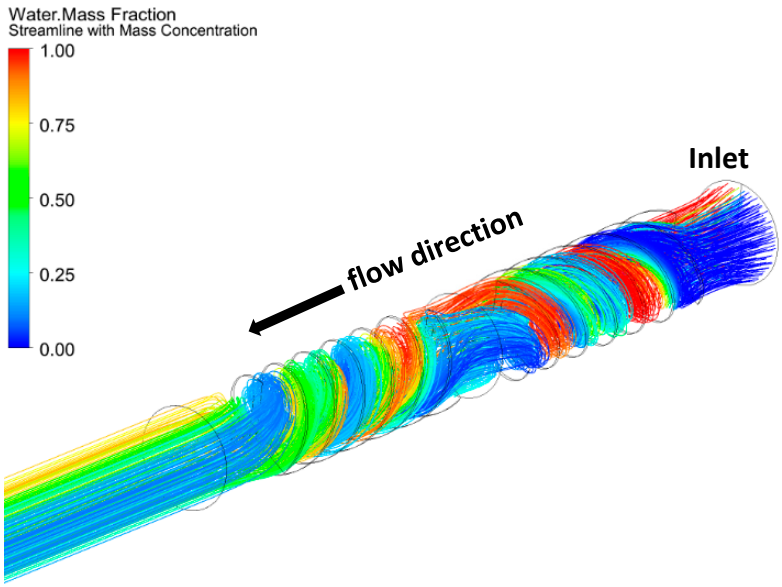

Figure 5: Typical mass concentration along streamlines (Re=Re_w=10).

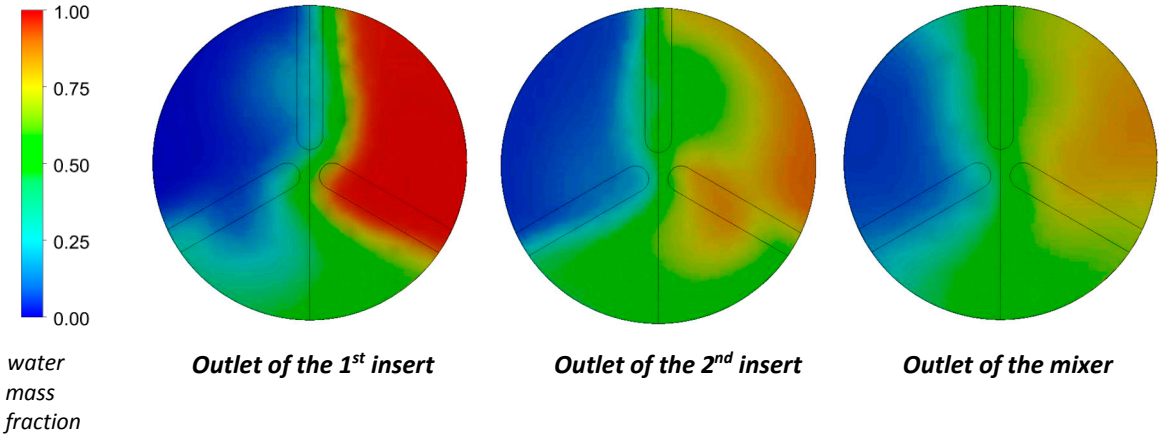

Figure 6: Mass fraction distribution at three cross sections of the device (Re=Re_w=10).

In Figure 7, the performance of the device is compared with that of a straight pipe whose cross section and length are the same as that of the proposed device. For a certain set of the design parameters and for the same Re number (Re_w=Re=10) the use of the mixing device configuration almost doubles the value of the I_{ME}. The increase of the fluid velocity considerably affects the mixing efficiency, or equally the uniformity of the mass fraction distribution at the exit of the device (Figure 8). It is evident that, as it is expected, the mixing efficiency is mainly influenced by the value of Re, or equally the velocity of the fluid, which leads to more intense swirling flow, despite the fact that at lower velocities the contact time of the fluids is longer.

Preprints (www.preprints.org) | NOT PEER-REVIEWED | Posted: 18 December 2017 doi:10.20944/preprints201712.0113.v1

Peer-reviewed version available at Fluids 2018, 3, 10; doi:10.3390/fluids3010010

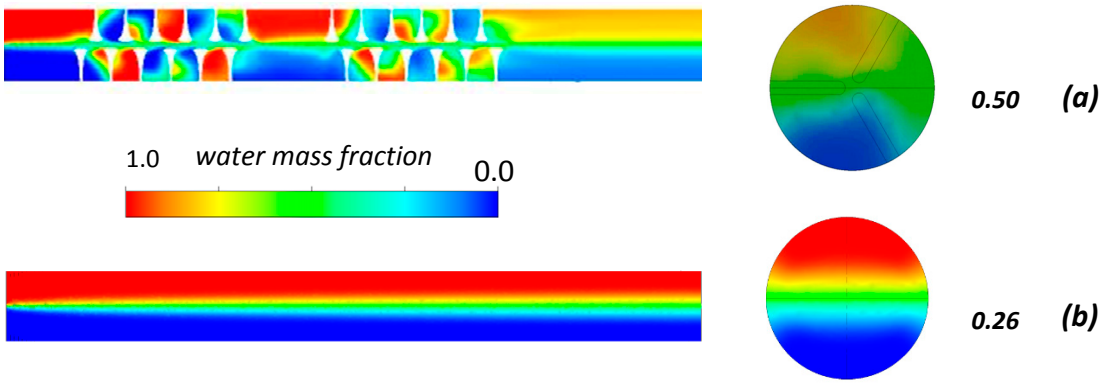

Figure 7: Comparison of the performance of the mixing device with that of a straight tube. Mass fraction distribution at a plane along the axis: a) of the device and b) of a straight pipe ($Re=Re_w=10$).

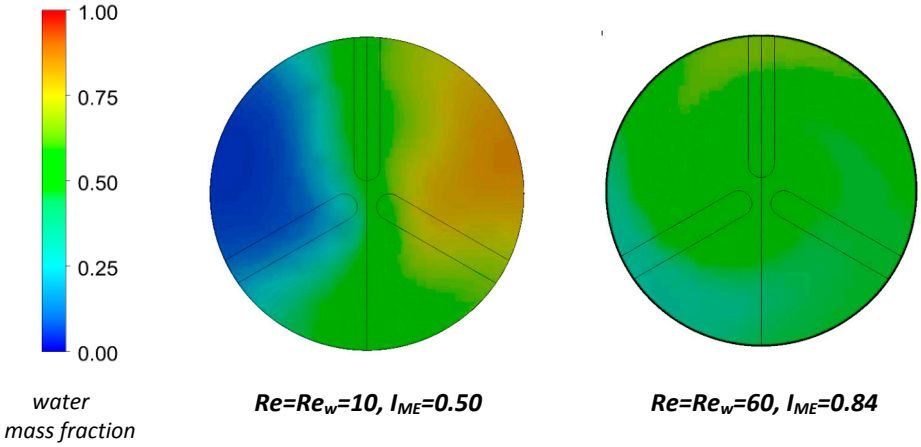

Figure 8: Effect of fluid velocity to the mixing efficiency at the outlet of the screening run device

3.2. Parametric study

The efficacy of the proposed mixing device was assessed by conducting a parametric study. However, to reduce the complexity of the problem some variables, namely the length and the inside diameter of the mixing device as well as the position, the length, the radius and the angle between the blades of the insert, were kept constant (as presented in Table 1). Also, for the sake of simplicity, the physical properties of one of the mixing fluids were assumed to be those of water, while the properties of the second fluid are variable and correspond to those of various types of water-based inks. Table 2 presents the independent, dimensionless variables involved in the parametric study as discussed above together with their upper and lower bound values. Based on the values used, Re/Re_w varies between 0.05 and 1.60.

The effect of the design parameters on the efficiency of the μ-device is investigated by performing a series of simulations for certain values of the design parameters chosen by employing the Box-Behnken method, i.e. an established Design-of-Experiments (DOE) techniques that allows the designer to extract as much information as possible from a limited number of test cases [12]. For the present study the number of design points dictated by the Box-Benken method is 42.

Preprints (www.preprints.org) | NOT PEER-REVIEWED | Posted: 18 December 2017 doi:10.20944/preprints201712.0113.v1

Peer-reviewed version available at Fluids 2018, 3, 10; doi:10.3390/fluids3010010

Table 2: Constraints of the design variables.

Parameter	Lower bound	Upper bound
Number of turns, n	1	3
Blockage ratio, l/D	0.2	0.58
Dynamic viscosity ratio, μ/μ_w	1.0	20
Density ratio, ρ/ρ_w	0.6	1.0
Inlet velocity ratio, u/u_w	1.0	3.0

Table 3: Design points for the simulation runs based on Box-Behnken DOE methodology.

run#	*turns, n*	*l/D*	μ/μ_w	ρ/ρ_w	u/u_w
DP01	3	0.20	10.5	0.8	2
DP02	1	0.20	10.5	0.8	2
DP03	1	0.39	10.5	0.6	2
DP04	1	0.39	1.0	0.8	2
DP05	1	0.39	10.5	0.8	1
DP06	1	0.39	10.5	0.8	3
DP07	1	0.39	20.0	0.8	2
DP08	1	0.39	10.5	1.0	2
DP09	1	0.58	10.5	0.8	2
DP10	2	0.20	10.5	0.6	2
DP11	2	0.20	1.0	0.8	2
DP12	2	0.20	10.5	0.8	1
DP13	2	0.20	10.5	0.8	3
DP14	2	0.20	20.0	0.8	2
DP15	2	0.20	10.5	1.0	2
DP16	2	0.39	1.0	0.6	2
DP17	2	0.39	10.5	0.6	1
DP18	2	0.39	10.5	0.6	3
DP19	2	0.39	20.0	0.6	2
DP20	2	0.39	1.0	0.8	1
DP21	2	0.39	1.0	0.8	3
DP22	2	0.39	10.5	0.8	2
DP23	2	0.39	20.0	0.8	1
DP24	2	0.39	20.0	0.8	3
DP25	2	0.39	1.0	1.0	2
DP26	2	0.39	10.5	1.0	1
DP27	2	0.39	10.5	1.0	3
DP28	2	0.39	20.0	1.0	2
DP29	2	0.58	10.5	0.6	2
DP30	2	0.58	1.0	0.8	2
DP31	2	0.58	10.5	0.8	1
DP32	2	0.58	10.5	0.8	3
DP33	2	0.58	20.0	0.8	2
DP34	2	0.58	10.5	1.0	2
DP35	3	0.39	10.5	0.6	2
DP36	3	0.39	1.0	0.8	2
DP37	3	0.39	10.5	0.8	1
DP38	3	0.39	10.5	0.8	3
DP39	3	0.39	20.0	0.8	2
DP40	3	0.39	10.5	1.0	2
DP41	3	0.58	10.5	0.8	2
DP42	2	0.20	10.5	0.8	2

The generic form of a fully quadratic model with two design parameters, x_1 and x_2, is the following:

$$Y = a_{11}x_1^2 + a_{22}x_2^2 + a_1x_1 + a_2x_2 + a_{12}x_1x_2 \quad (3)$$

The model includes the quadratic, the linear terms, and their interaction. To avoid overfitting, it is important that the researcher addresses the importance of each factor of the model. Additionally, it is also significant to take into account any possible insight regarding the potential form of the final equation and its non-linearity. For this reason, a different approach is followed in this case: the fitting approach uses the natural logarithms of the design parameters and responses. Based on the outcome, it is safe, within a certain degree of acceptable error, to ignore the quadratic terms and fit a model with only the linear terms and some of their interactions.

The following equation represents the proposed model:

Preprints (www.preprints.org) | NOT PEER-REVIEWED | Posted: 18 December 2017 doi:10.20944/preprints201712.0113.v1

Peer-reviewed version available at Fluids 2018, 3, 10; doi:10.3390/fluids3010010

$$\ln(Y) = \alpha \ln(n) + \beta \ln\left(\frac{l}{D}\right) + \gamma \ln\left(\frac{\mu}{\mu_w}\right) + \delta \ln\left(\frac{\rho}{\rho_w}\right) + \varepsilon \ln\left(\frac{u}{u_w}\right) + \zeta \ln\left(\frac{l}{D}\right) \ln\left(\frac{l}{D}\right) + \eta \ln(n) \ln\left(\frac{\mu}{\mu_w}\right) + \theta \ln\left(\frac{l}{D}\right) \ln\left(\frac{\mu}{\mu_w}\right) + \iota \ln\left(\frac{u}{u_w}\right) \ln\left(\frac{\mu}{\mu_w}\right) + cst \quad (4)$$

whose parameters can be calculated with regression based on response surface methodology; Y is the response, i.e. ΔP or I_{ME}, and cst is a constant. The annexed form of the final model would then be:

$$Y = n^{\alpha} \left(\frac{l}{D}\right)^{\beta+\zeta \ln\left(\frac{l}{D}\right)} \left(\frac{\mu}{\mu_w}\right)^{\gamma+\eta \ln(n)+\theta \ln\left(\frac{l}{D}\right)+\iota \ln\left(\frac{u}{u_w}\right)} \left(\frac{\rho}{\rho_w}\right)^{\delta} \left(\frac{u}{u_w}\right)^{\varepsilon} e^{cst} \quad (5)$$

A transform of the above model to include the Re ratio instead of the velocity ratio would be:

$$\boldsymbol{Y = n^{\alpha} \left(\frac{l}{D}\right)^{\beta+\zeta \ln\left(\frac{l}{D}\right)} \left(\frac{\mu}{\mu_w}\right)^{\gamma+\eta \ln(n)+\theta \ln\left(\frac{l}{D}\right)+\iota \ln\left(\frac{Re\ \mu\ \rho_w}{Re_w \mu_w\ \rho}\right)+\varepsilon} \left(\frac{\rho}{\rho_w}\right)^{\delta-\varepsilon} \left(\frac{Re}{Re_w}\right)^{\varepsilon} e^{cst}} \quad (6)$$

Table 4 contains the parameters of the fitting models for ΔP and I_{ME} respectively.

Table 4: Response surface model parameters for a) ΔP & b) I_{ME}.

parameter	ΔP	IME
α	0.817014	0.026161
β	5.456162	-1.48235
γ	0.594749	-0.34662
δ	0.312127	-0.18884
ε	0.72966	-0.42494
ζ	1.472507	-0.99062
η	-0.02689	0.097432
θ	0.014815	-0.16046
ι	0.126574	0.092324
cst	5.91789	-0.66962

From Figure 9, where the values calculated using the proposed equations are compared with the CFD results, it is evident that they can predict with ±10% accuracy both ΔP (Figure 9a) and I_{ME} (Figure 9b) values. The validity of the proposed correlations is further examined by comparing them with CFD the results generated using the six "verification points" presented in Table 3 and are also in agreement (Figure 9).

Table 5: Verification points

run#	*turns, n*	*l/D*	μ/μ_w	ρ/ρ_w	u/u_w
VP01	3	0.20	10.5	0.8	2
VP02	1	0.20	10.5	0.8	2
VP03	1	0.39	10.5	0.6	2
VP04	1	0.39	1.0	0.8	2
VP05	1	0.39	10.5	0.8	1
VP06	1	0.39	10.5	0.8	3

Preprints (www.preprints.org) | NOT PEER-REVIEWED | Posted: 18 December 2017 doi:10.20944/preprints201712.0113.v1

Peer-reviewed version available at Fluids 2018, 3, 10; doi:10.3390/fluids3010010

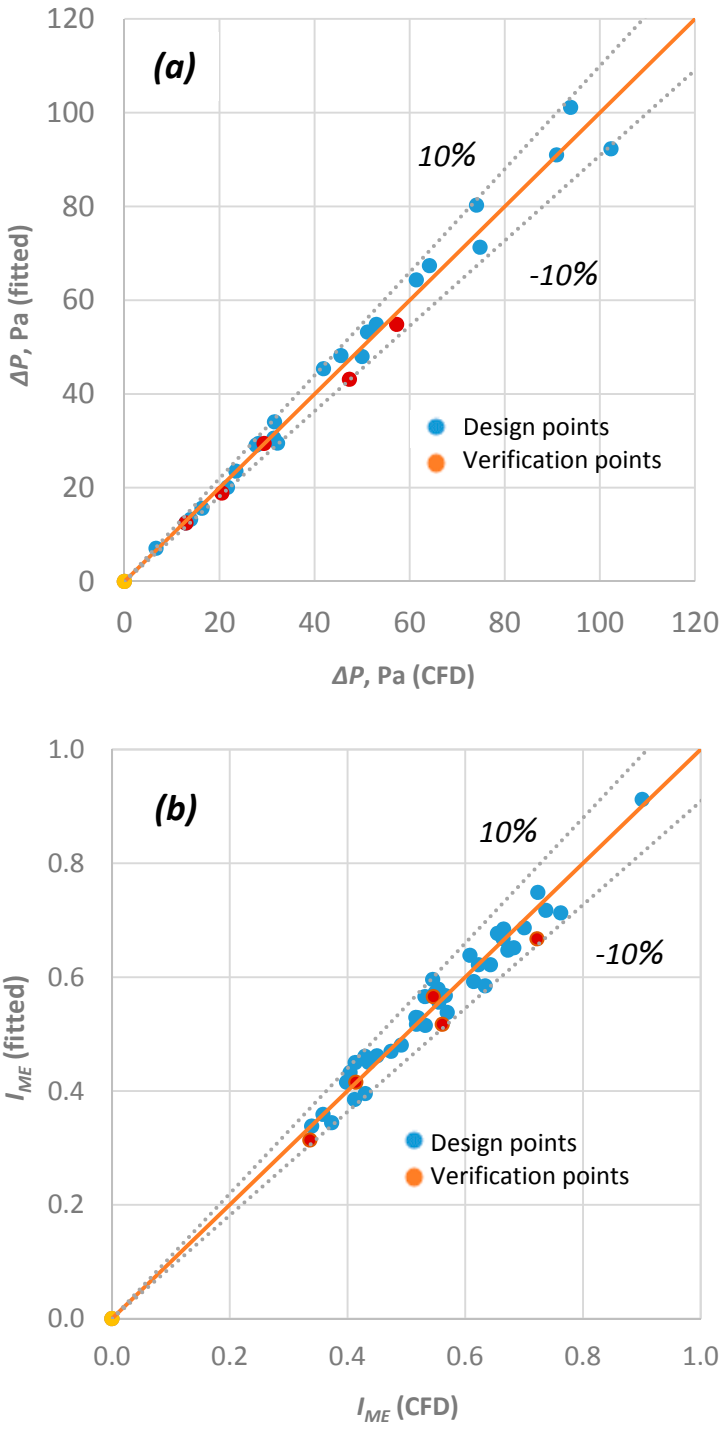

Figure 9: Comparison between CFD and fitted values for a) ΔP & b) I_{ME}.

4 Conclusions

In this study, we have numerically investigated the mixing efficiency as well as the corresponding ΔP inside a novel type of μ-mixer. The device comprises two successive helical inserts that propel the fluid to opposite directions and induces mixing by generating swirling flow. Screening experiments reveal that the addition of the second insert improves mixing considerably. It was also found that for the range of *Re* numbers investigated the resulting pressure drop is maintained at low levels (<150 Pa).

Preprints (www.preprints.org) | NOT PEER-REVIEWED | Posted: 18 December 2017 doi:10.20944/preprints201712.0113.v1

Peer-reviewed version available at Fluids 2018, 3, 10; doi:10.3390/fluids3010010

Appropriate "computational experiments" were then conducted to investigate the effect of the various geometrical parameters of the novel μ-mixer, i.e. the one with the two inserts, and the parameters of the mixing fluids (physical properties and flow rate) on the mixing performance of the proposed device. Both the number of the required "computational experiments" and the values of the design parameters were selecting using a DOE methodology. Using the data obtained from the "computational experiments" correlations, which are able to predict the mixing efficiency and the associated pressure drop with ±10% accuracy, have been formulated.

In the next stage of the study, experiments will be performed using a prototype helical insert that has been already constructed by 3D printing (Figure 10). The experimental data acquired using the device will be used for evaluating the CFD code. The aim is to provide a means of constructing the type of helical insert that would be more suitable for a given application.

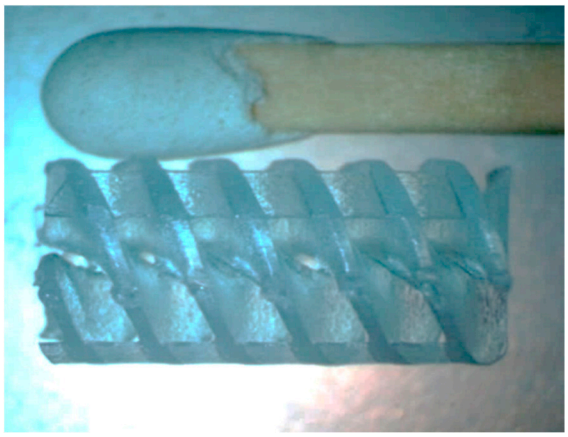

Figure 10: The helical insert constructed by 3D printing.

Acknowledgements: The authors would like to thank Prof. S.V. Paras for his constructive comments.

Author Contributions: A.A. Mouza had the initial conception of this work; A.G. Kanaris and A.A. Mouza designed the CFD experiments, performed the simulations, acquired and analyzed the data and interpreted the results; A.G. Kanaris drafted the work and A.A. Mouza revised the manuscript.

Conflicts of Interest: All authors state that there is no conflict of interest.

Nomenclature

A	cross-section of the device	mm^2
b	blade pitch	mm
c	mass fraction in each cell of a cross-section A	dimensionless
$\bar{c}$	mean concentration over a cross-section A	dimensionless
D	diameter of the insert	mm
D_m	inside diameter of the device	mm
I_{ME}	Index of Mixing Efficiency	dimensionless
l	blade length	mm
L	length of the insert	mm
L_m	total length of mixer	mm
n	number of turns of the insert	dimensionless
Re	Reynolds number of each liquid based on D	dimensionless
ΔP	pressure drop	Pa
μ	liquid viscosity	Pa s

Preprints (www.preprints.org) | NOT PEER-REVIEWED | Posted: 18 December 2017 doi:10.20944/preprints201712.0113.v1

Peer-reviewed version available at Fluids 2018, 3, 10; doi:10.3390/fluids3010010

ρ	liquid density	kg/m^3
ϕ	angle between blade	deg

References

1. Nguyen, N.T., Wu, Z. Micromixers—a review. Journal of Micromechanics and Microengineering 2005, 15.
2. Hardt, S., Drese, K.S. Passive micromixers for applications in the microreactor and μTAS fields. Microfluidics and Nanofluidics 2005, 1, 108-118, 10.1007/s10404-004-0029-0.
3. Hessel, V., Löwe, H., Schönfeld, F. Micromixers—a review on passive and active mixing principles. Chemical Engineering Science 2005, 60, 2479-2501, https://doi.org/10.1016/j.ces.2004.11.033.
4. Mansur, E.A., Ye, M. A State-of-the-Art Review of Mixing in Microfluidic Mixers. Chinese Journal of Chemical Engineering 2008, 16, 503-516, https://doi.org/10.1016/S1004 - 9541(08)60114-7.
5. Kanaris, A.G., Stogiannis, I.A. Comparing the mixing performance of common types of chaotic micromixers: A numerical study. Heat Transfer Engineering 2015, 36, 1122-1131, 10.1080/01457632.2015.987623.
6. Mouza, A.A., Patsa, C.M., Schönfeld, F. Mixing performance of a chaotic micro-mixer. Chemical Engineering Research and Design 2008, 86, 1128-1134, 10.1016/j.cherd.2008.04.009.
7. Kanaris, A.G.,Mouza, A.A. Numerical investigation of the effect of geometrical parameters on the performance of a micro-reactor. Chemical Engineering Science 2011, 66, 5366-5373, 10.1016/j.ces.2011.07.044.
8. Huang, S.-W., Wu, C.-Y. Fluid mixing in a swirl-inducing microchannel with square and T-shaped cross-sections. Microsystem Technologies 2017, 23, 1971-1981, 10.1007/s00542-016-2952-x.
9. Rawool, A.S., Mitra, S.K., Kandlikar, S.G. Numerical simulation of flow through microchannels with designed roughness. Microfluidics and Nanofluidics 2006, 2, 215-221, 10.1007/s10404-005-0064-5.
10. Pahl, M.H., Muschelknautz, E. Static mixers and their applications, Inter. Chem. Eng, 1982.
11. Versteeg H.,K., Malalasekera, W. Computational fluid dynamics Longman Press, London, UK, 1995.
12. Box, G.E.P., Hunter, J.S.,Hunter, W.G. Statistics for Experimenters: Design, Innovation and Discovery, Second Edition ed, J. Wiley and Sons, Inc, 2005.